Realization of balanced gain and loss in a time-dependent four-mode Bose-Hubbard model

Daniel Dizdarevic,* Jörg Main, Kirill Alpin, Johannes Reiff, Dennis Dast, Holger Cartarius, and Günter Wunner
Institut für Theoretische Physik 1, Universität Stuttgart, 70550 Stuttgart, Germany

(Received 16 October 2017; published 22 January 2018)

A quantum system exhibiting $\mathcal{PT}$ symmetry is a Bose-Einstein condensate in a double-well potential with balanced particle gain and loss, which is described in the mean-field limit by a Gross-Pitaevskii equation with a complex potential. A possible experimental realization of such a system by embedding it into a Hermitian time-dependent four-mode optical lattice was proposed by Kreibich *et al.* [Phys. Rev. A **87**, 051601(R) (2013)], where additional potential wells act as reservoirs and particle exchange happens via tunneling. Since particle influx and outflux have to be controlled explicitly, a set of conditions on the potential parameters had to be derived. In contrast to previous work, our focus lies on a full many-body description beyond the mean-field approximation using a Bose-Hubbard model with time-dependent potentials. This gives rise to additional quantum effects, such that the differences between mean-field and many-body dynamics are of special interest. We further present stationary *analytical* solutions for the embedded wells in the mean-field limit, different approaches for the embedding into a many-body system, and a very efficient method for the evaluation of hopping terms to calculate exact Bose-Hubbard dynamics.

DOI: 10.1103/PhysRevA.97.013623

I. INTRODUCTION

In recent years a growing interest in non-Hermitian and especially $\mathcal{PT}$-symmetric quantum mechanics has arisen, since such theories allow for an effective description of open quantum systems [1]. $\mathcal{PT}$ symmetry [2], meaning that the Hamiltonian is invariant under combined parity and time reflection, has already been observed in optical systems [3–6], microwave cavities [7], and electronics [8].

A well-investigated and experimentally accessible genuine quantum system exhibiting $\mathcal{PT}$ symmetry was proposed by Klaiman *et al.* [9] and is given by a Bose-Einstein condensate (BEC) in a double-well potential with balanced gain and loss (BGL) [10–16]. In theory, gain and loss can be introduced via complex potentials [17] or Lindblad superoperators [18]. Although such descriptions render the Hamiltonian non-Hermitian, in the $\mathcal{PT}$-symmetric case stationary states with real eigenvalues exist.

Experimental techniques for the realization of gain and loss are well developed these days. Localized gain can be realized by feeding atoms from a second condensate [19,20], while localized loss can be achieved with a focused electron beam [21–23]. Although the experimental tools for a direct realization of $\mathcal{PT}$-symmetric BECs are in principle available, no such experiment has been accomplished so far. Other realizations of $\mathcal{PT}$-symmetric systems in ultracold atoms were proposed by means of bound wave functions [24,25], and recently experiments were performed using only localized loss, which, however, effectively show BGL [26]. There are also theoretical investigations of the double-well system beyond a Gross-Pitaevskii dynamics, where the open quantum system is described by a Lindblad-type master equation [27,28].

Here, however, we focus on yet another approach; that is, an embedding of a two-mode BEC in a larger Hermitian system [29,30] allowing for a causal description of particle gain and loss via tunneling. To this end, parameters of the optical lattice have to be varied in a time-dependent manner based on the current state of the system. While this method is already theoretically well investigated within the mean-field (MF) approximation even for large particle numbers [31], which is in principle sufficient for the description of a potential experiment, we are particularly interested in a many-body description of such systems. By consideration of two-mode models, additional generic quantum effects in open many-body systems were found, e.g., purity oscillations [28,32], which are experimentally manifested in the average contrast [33]. To experimentally investigate such effects, BGL has to be established over sufficiently long timescales. This makes a many-body realization of the two-mode model in the low-particle-number limit of particular interest, which will be the main topic of this paper.

This paper is organized as follows: We will start by giving a short overview of the Bose-Hubbard (BH) model and a discussion about different approximations in Sec. II. Afterwards, in Sec. III, we will introduce the $\mathcal{PT}$-symmetric two-mode model and its embedding into a four-mode optical lattice in the MF. We transfer these results to many-body systems in Sec. IV by also employing time-dependent potentials in the BH model. It will be discussed in detail whether $\mathcal{PT}$ symmetry or BGL as known from the MF can still be observed in a double-well system embedded into an optical lattice by using a full many-body description. Finally, we give some conclusions and an outlook in Sec. V.

II. MODELS AND METHODS FOR MANY-BODY SYSTEMS

In this section we recapitulate the basic concepts and methods necessary for a many-body description of optical

*daniel.dizdarevic@itp1.uni-stuttgart.de

lattice systems. The equations discussed here are valid for any M-mode optical lattice and lay the foundation for the following sections, where we will consider the special case of four-mode optical lattice systems.

A. Bose-Hubbard model

The BH model [34] is a model for the description of the many-body dynamics of trapped bosons in multiwell potentials, such as ultracold atoms in optical lattices [35]. The BH Hamiltonian for an M-well system reads

$$\mathcal{H}_{\mathrm{BH}}(t) = -\sum_{\langle m,m'\rangle} J_{mm'}(t)\hat{a}_m^\dagger \hat{a}_{m'} + \frac{1}{2}\sum_m U_m(t)\hat{n}_m(\hat{n}_m - 1) + \sum_m \mu_m(t)\hat{n}_m, \tag{1}$$

where $\langle\cdot,\cdot\rangle$ denotes the summation of all nearest neighbors for $m,m' \in [1,M]$. The operators $\hat{a}_m^\dagger$ and $\hat{a}_m$ are the bosonic particle creation and annihilation operators for well m and $\hat{n}_m = \hat{a}_m^\dagger \hat{a}_m$ denotes the corresponding particle number operator.

The first term is the kinetic part of the BH Hamiltonian, which describes particle exchange between nearest neighbors with rates $J_{mm'}$, whereas the second and third terms are the potential energies due to contact interactions U_m and chemical potentials μ_m in each well, respectively; the last term in Eq. (1) is therefore also called *on-site energy*.

It should be noted at this point that the parameters in our model are explicitly time-dependent in contrast to most other applications. This is due to the fact that we will later use the potential parameters $J_{mm'}$ and μ_m to control the dynamics in the system. Thus, the interaction energy U_m is time dependent as well, since it involves an overlap integral of the wave function at one site [35]. However, for the sake of simplicity we only consider the case where $U_m(t) = U$ is constant and equal at each site. Considering only s-wave scattering, where the parameter U depends on the scattering length a as described in Ref. [35], this assumption corresponds to a dynamical $a(t)$, which is realizable by Feshbach resonances [36,37]. Nevertheless, the method presented in the following sections is still applicable in the general case of Eq. (1) by appropriate modifications, although, no change in the qualitative behavior is expected.

A natural basis for the M-mode BH model is formed by the Fock states $|n_1,\ldots,n_M\rangle$ with $\sum_{k=1}^M n_k = N$. Although our BH model (1) explicitly contains time-dependent potentials we can still resort to standard methods to calculate its exact time evolution and dynamics (see, e.g., Ref. [38]) while using a slightly advanced method for evaluating the hopping terms. After a pairwise application of creation and annihilation operators, we calculate the position of the resulting vector in a lexicographically ordered basis directly as shown in the appendix. Since most matrix elements contain time-dependent parameters and therefore depend on the current state of the system, matrix multiplications have to be evaluated on the fly.

B. Approximations to the Bose-Hubbard model

The dimension of the Fock basis scales roughly as N^{M-1} for $N \gg 1$ [cf. Eq. (A1)] and grows rapidly with an increasing number of particles, thus restricting the numerical computations for exact many-body dynamics to particle numbers $N \lesssim 200$. To enter the larger-particle-number regime, in the following we briefly discuss different approximations to the BH model.

The simplest approximation possible is the well-known MF approximation (see, e.g., Ref. [39]), where the dynamics is given by the average behavior of all particles in the ground state. With the notation $\psi_m = \langle\psi_0|\hat{a}_m|\psi_0\rangle$ and for $N \gg 1$ the Heisenberg equations of motion for annihilation and creation operators yield

$$i\frac{\partial}{\partial t}\psi_m = -J_{m,m-1}\psi_{m-1} - J_{m,m+1}\psi_{m+1} + U_m n_m \psi_m + \mu_m \psi_m, \tag{2}$$

which is the discrete Gross-Pitaevskii equation (GPE) [40,41], also obtainable from the continuous GPE via a frozen Gaussian ansatz [30,42–44]. This MF approximation describes the dynamics of a BEC in the limit $N \to \infty$ and $T \to 0$, where the occupation of the ground state is dominant. However, there is a huge downside; every particle is assumed to be in the same single-particle state and thus all many-particle information about the interacting system is lost completely.

An approximation beyond the MF for the treatment of large numbers of particles is the so-called Bogoliubov back-reaction (BBR) method [45–47]. By using the density operator $\hat{\rho}$, the full many-body dynamics described by the BH model (1) can be rewritten in terms of the expectation values of the entries of the single-particle density matrix (SPDM) $\sigma_{ij}^{(1)} = \langle\hat{a}_i^\dagger \hat{a}_j\rangle$, the two-particle density matrix (TPDM) $\sigma_{ijkl}^{(2)} = \langle\hat{a}_i^\dagger \hat{a}_j \hat{a}_k^\dagger \hat{a}_l\rangle$, or, in general, the n-particle density matrices

$$\sigma_{i_1\ldots i_n}^{(n)} = \langle\hat{a}_{i_1}^\dagger \hat{a}_{i_1}\cdots\hat{a}_{i_n}^\dagger \hat{a}_{i_n}\rangle. \tag{3}$$

The first two orders of this Bogoliubov–Born–Green–Kirkwood–Yvon-type (BBGKY-type) hierarchy [46] read

$$i\frac{\partial}{\partial t}\sigma_{ij}^{(1)} = \mathcal{Z}_{ij}^{(1)} - (\mu_i - \mu_j)\sigma_{ij}^{(1)}, \tag{4a}$$

$$i\frac{\partial}{\partial t}\sigma_{ijkl}^{(2)} = \mathcal{Z}_{ijkl}^{(2)} - (\mu_i - \mu_j + \mu_k - \mu_l)\sigma_{ijkl}^{(2)}, \tag{4b}$$

where, for later purposes, we define

$$\mathcal{Z}_{ij}^{(1)} = J_{i-1,i}\sigma_{i-1,j}^{(1)} + J_{i+1,i}\sigma_{i+1,j}^{(1)} - J_{j,j-1}\sigma_{i,j-1}^{(1)} - J_{j,j+1}\sigma_{i,j+1}^{(1)} - U\left(\sigma_{iiij}^{(2)} - \sigma_{ijjj}^{(2)}\right), \tag{4c}$$

$$\begin{aligned}\mathcal{Z}_{ijkl}^{(2)} = {} & J_{i-1,i}\sigma_{i-1,jkl}^{(2)} + J_{i+1,i}\sigma_{i+1,jkl}^{(2)} \\ & - J_{j,j-1}\sigma_{i,j-1,kl}^{(2)} - J_{j,j+1}\sigma_{i,j+1,kl}^{(2)} \\ & + J_{k-1,k}\sigma_{ij,k-1,l}^{(2)} + J_{k+1,k}\sigma_{ij,k+1,l}^{(2)} \\ & - J_{l,l-1}\sigma_{ijk,l-1}^{(2)} - J_{l,l+1}\sigma_{ijk,l+1}^{(2)} \\ & - U\left(\sigma_{iiijkl}^{(3)} - \sigma_{ijjjkl}^{(3)} + \sigma_{ijkkkl}^{(3)} - \sigma_{ijklll}^{(3)}\right).\end{aligned} \tag{4d}$$

It should be noted that the nth order in this hierarchy is coupled to the $(n+1)$st order by the contact-interaction strength, where $n < N$, with the total number of particles N in the system.

Now the BBR approximation [45–47] comes into play cutting off the hierarchy (4) after the second-order such that

a closed system of coupled differential equations is formed. Following Ref. [47], we start with

$$\hat{\sigma}_{ij}^{(1)} \approx \sigma_{ij}^{(1)} + \delta\hat{\sigma}_{ij}^{(1)}. \tag{5}$$

To uncouple Eqs. (4) from the remaining dynamics, one has to expand $\sigma_{ijklmn}^{(3)}$ using Eq. (5), which yields

$$\sigma_{ijklmn}^{(3)} \approx \sigma_{ij}^{(1)}\sigma_{klmn}^{(2)} + \sigma_{mn}^{(1)}\sigma_{ijkl}^{(2)} + \sigma_{kl}^{(1)}\sigma_{ijmn}^{(2)} - 2\sigma_{ij}^{(1)}\sigma_{kl}^{(1)}\sigma_{mn}^{(1)}. \tag{6}$$

Apart from the single-particle dynamics, this BBR method also contains two-particle dynamics, which is the most significant many-body contribution beyond the MF dynamics. In principle, even better BBR approximations are possible by cutting off the hierarchy at higher orders; however, the computational cost increases exponentially.

The BBR approximation and the BBGKY hierarchy in general feature a specific symmetry; that is,

$$\left(\sigma_{k\cdots l}^{(n)}\right)^* = \sigma_{l\ldots k}^{(n)}, \tag{7}$$

i.e., a complex conjugation will reverse the order of the indices. This comes in handy to reduce computational effort to some extent.

III. REALIZATION OF TWO-MODE MODEL IN MEAN FIELD

In the following section we will introduce the $\mathcal{PT}$-symmetric two-mode model in the MF approximation. Then, the basic concept of embedding this open quantum system into a larger Hermitian system is discussed for a four-mode system. We derive fundamental conditions for the embedding and analytical solutions for stationary states.

A. $\mathcal{PT}$-symmetric two-mode model

The dynamics of a BEC at very low temperatures and in the limit of large particle numbers is well described by the GPE. If the wells of the trapping potential are sufficiently deep, the GPE can be reduced to a matrix model [cf. Eq. (2)] [14,29,30]. In the case of a $\mathcal{PT}$-symmetric double-well potential [10], the dimensionless discrete GPE reads [14]

$$i\frac{\partial}{\partial t}\begin{pmatrix}\psi_1\\ \psi_2\end{pmatrix} = \begin{pmatrix} g|\psi_1|^2 + i\gamma & -J_{12}\\ -J_{12} & g|\psi_2|^2 - i\gamma\end{pmatrix}\begin{pmatrix}\psi_1\\ \psi_2\end{pmatrix}, \tag{8}$$

where

$$\psi_k = \sqrt{n_k}\exp(i\varphi_k) \tag{9}$$

are complex numbers describing the MF wave function at site k. The macroscopic interaction strength

$$g = (N-1)U \tag{10}$$

describes contact interactions for N particles with interaction energy U as in Eq. (1) and vanishes for a single particle, i.e., $N = 1$. In the MF, i.e., for a large number of particles, $(N - 1) \sim N$ can be used; we are, however, interested in the low-particle-number limit. Particle exchange between neighboring sites is given by the off-diagonal elements of the Hamiltonian with tunneling constants $J_{12} \geqslant 0$, while particle exchange with the environment is described by an antisymmetric imaginary potential with coupling strength γ. This non-Hermitian two-mode model on the one hand shows $\mathcal{PT}$-symmetric stationary states with completely real eigenvalues and nonzero current, and on the other hand $\mathcal{PT}$-broken states with complex eigenvalues [14] as well as rich bifurcation schemes [10–13]. For sufficiently small values of γ and g, the eigenvalue spectrum is real and there exist $\mathcal{PT}$-symmetric stationary solutions to Eq. (8).

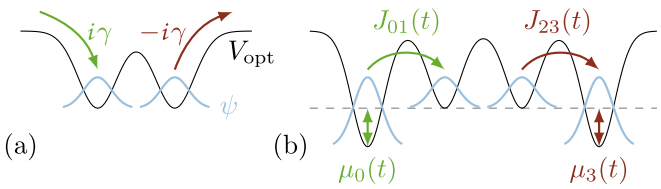

FIG. 1. (a) Open non-Hermitian two-mode system and (b) closed Hermitian four-mode system. The currents between the outer reservoir wells and the inner wells account for the in- and out-coupling of particles in the open quantum system. To reproduce the properties of an open system the additional parameters $J_{01}(t)$, $J_{23}(t)$, $\mu_0(t)$, and $\mu_3(t)$ have to be varied time dependently.

B. Embedding into a four-mode system

Although the $\mathcal{PT}$-symmetric two-mode model (8) is quite simple, so far there was no observation of $\mathcal{PT}$ symmetry in a real quantum system because such an open quantum system is hard to realize experimentally. For this reason, we rely on Ref. [29] and, as shown in Fig. 1, embed the two-mode model into a four-mode optical potential, which can be painted in a time-averaged manner by using a rapidly moving laser beam [48]. Although there is a method available for creating an actual loss as described by an imaginary potential $-i\gamma$ by using an electron beam [23,26,49], we want to focus completely on the realization of an open quantum system via the approach of embedding it into a larger structure, where the reservoir is explicitly modeled and controlled.

By embedding a two-mode system into a larger Hermitian system, we allow for particle and energy exchange between the two-mode subsystem, in the following simply referred to as the *embedded system*, and the additional *reservoir wells*. While one additional well at each side of the system is sufficient for the embedding, such a reservoir will in general not fulfill the Markov property. Markovian behavior, i.e., memorylessness of the environment, is a fundamental assumption underlying the $\mathcal{PT}$-symmetric two-mode model and its many-body counterpart given by a Lindblad-type master equation. For large population numbers, however, the finite size of the reservoir becomes less significant. Systems with a large number of reservoir wells were investigated in Ref. [31] for the MF case.

While also the four-mode system has already been studied intensively [29,30], we will not only recap these previous results, but rather rework the MF problem in order to lay the foundation for Sec. IV. Although those previous results are in principle applicable to many-body systems, their complexity provides difficulties. Therefore, it is required to discuss the MF theory, although our intention is to go beyond MF in the present paper. Moreover, by directly using the equations of motion for the SPDMs $\sigma_{ij} = \psi_i^*\psi_j$, which will be seen

later is a natural approach to also employ the results in many-body calculations, a degree of freedom $d(t)$ remains, i.e., an arbitrary time-dependent function, which does not change the observables at all. We, however, eliminate this degree of freedom by using the equations of motion for the macroscopic wave function ψ instead, which will also yield much simpler results in terms of complexity as will be shown in this section. For those who are familiar with Ref. [30], although, we want to mention that our results are in fact fully equivalent to their results for the unique functional relation

$$d(t) = -\frac{J_{12}}{2\sqrt{n_0(t)n_3(t)}}. \tag{11}$$

To emulate the in- and out-coupling of particles in analogy with the effects of a complex potential in the embedded system, we have to control the tunneling processes by altering the additional parameters of the optical potential in the reservoir wells in a time-dependent manner; namely, $J_{01}(t)$, $J_{23}(t)$, $\mu_0(t)$, and $\mu_3(t)$. To this end, the dynamics of the $\mathcal{PT}$-symmetric two-mode model (8) is compared with the embedded dynamics in a time-dependent four-mode model with the Hamiltonian

$$\begin{pmatrix} g|\psi_0|^2+\mu_0(t) & -J_{01}(t) & 0 & 0 \\ -J_{01}(t) & g|\psi_1|^2 & -J_{12} & 0 \\ 0 & -J_{12} & g|\psi_2|^2 & -J_{23}(t) \\ 0 & 0 & -J_{23}(t) & g|\psi_3|^2+\mu_3(t) \end{pmatrix}, \tag{12}$$

which immediately yields the complex-valued conditions

$$J_{01}\psi_0 = -i\gamma\psi_1, \tag{13a}$$

$$J_{23}\psi_3 = i\gamma\psi_2. \tag{13b}$$

A remarkable feature of these conditions is the necessity of a defined antisymmetric phase relation between system and reservoir wells,

$$\varphi_0 - \varphi_1 = -\frac{\pi}{2}, \tag{14a}$$

$$\varphi_3 - \varphi_2 = \frac{\pi}{2}, \tag{14b}$$

which is a consequence of the definition (9). If these phase relations hold, in- and out-coupling of particles can indeed be realized by particle currents and the time-dependent tunneling rates are given by

$$J_{01}(t) = \frac{2\gamma n_1(t)}{\tilde{j}_{01}(t)}, \tag{15a}$$

$$J_{23}(t) = \frac{2\gamma n_2(t)}{\tilde{j}_{23}(t)}, \tag{15b}$$

where we introduced the reduced current density

$$\tilde{j}_{ij} = 2\,\mathrm{Im}(\psi_i^*\psi_j), \tag{16}$$

such that $j_{ij} = J_{ij}\tilde{j}_{ij}$ describes the current between wells i and j. Analogously we also introduce

$$c_{ij} = 2\,\mathrm{Re}(\psi_i^*\psi_j) \propto \cos(\varphi_i - \varphi_j), \tag{17}$$

such that, with Eqs. (14),

$$c_{01} = c_{23} = 0. \tag{18}$$

As the previous considerations show, the embedding critically depends on the conservation of specific phase relations. To ensure the validity of Eqs. (14), it is sufficient to demand that they hold initially and $\dot{c}_{01} = \dot{c}_{23} = 0$ for all times t, which yields

$$\mu_0(t) = -J_{12}\frac{\tilde{j}_{02}(t)}{\tilde{j}_{01}(t)} - g[n_0(t) - n_1(t)], \tag{19a}$$

$$\mu_3(t) = -J_{12}\frac{\tilde{j}_{13}(t)}{\tilde{j}_{23}(t)} - g[n_3(t) - n_2(t)]. \tag{19b}$$

With the time-dependent parameters (15) and (19), the dynamics of the embedded wells resembles the dynamics of the open quantum system (8) for all initial states satisfying the phase relations (14), which is in agreement with the previous results from Refs. [29,30] using Eq. (11).

In the following, we consider quasistationary states of the four-mode model, i.e., steady states of the embedded system corresponding to $\mathcal{PT}$-symmetric states in the two-mode model [14]. Such states arise from the initial conditions

$$n_1(0) = n_2(0) = n, \tag{20a}$$

$$j_{01}(0) = j_{12}(0) = j_{23}(0) = 2\gamma n. \tag{20b}$$

Without loss of generality, the initial conditions for the MF wave function read

$$\psi_0(0) = \sqrt{n_0(0)}\exp[i(\varphi - \pi/2)], \tag{21a}$$

$$\psi_1(0) = \sqrt{n}\exp(i\varphi), \tag{21b}$$

$$\psi_2(0) = \sqrt{n}\exp(-i\varphi), \tag{21c}$$

$$\psi_3(0) = \sqrt{n_3(0)}\exp[-i(\varphi - \pi/2)], \tag{21d}$$

with

$$\varphi = -\frac{1}{2}\arcsin\left(\frac{\gamma}{J_{12}}\right). \tag{21e}$$

If we demand constant gain and loss, i.e., γ is constant, the conditions (20) are preserved for all times. Therefore, the occupation numbers in the reservoir will change linearly in time,

$$n_0(t) = n_0(0) - 2\gamma n t, \tag{22a}$$

$$n_3(t) = n_3(0) + 2\gamma n t. \tag{22b}$$

Equations (14), (20), and (22) can be used to obtain analytical expressions for the time-dependent lattice parameters,

$$J_{01}(t) = \gamma\sqrt{\frac{n}{n_0(0) - 2\gamma n t}}, \tag{23a}$$

$$J_{23}(t) = \gamma\sqrt{\frac{n}{n_3(0) + 2\gamma n t}}, \tag{23b}$$

$$\mu_0(t) = \mu - g[n_0(0) - 2\gamma n t], \tag{23c}$$

$$\mu_3(t) = \mu - g[n_3(0) + 2\gamma n t], \tag{23d}$$

where the chemical potential μ is given by

$$\mu = gn - \sqrt{J_{12}^2 - \gamma^2}. \tag{23e}$$

Note that these analytical results go beyond Refs. [29,30].

A remarkable feature of Eqs. (23) is that initial populations in the reservoir wells can be chosen arbitrarily. However, the choice of $n_0(0)$ determines the timescale on which quasistationary states can be realized, i.e., the system breaks down when the left reservoir is empty at time

$$\tau = \frac{n_0(0)}{2\gamma n}. \tag{24}$$

To summarize, by means of time-dependent parameters, stationary states and therefore $\mathcal{PT}$ symmetry can be realized in the embedded system for $0 \leqslant t \leqslant \tau$ within the MF approximation, i.e., the inner wells of the Hermitian four-mode system (12) behave exactly as the non-Hermitian two-mode system (8).

IV. RESULTS AND DISCUSSION

It was shown in Sec. III that the $\mathcal{PT}$-symmetric two-mode model can be realized in the MF by using a time-dependent four-mode optical lattice. Naturally the question arises whether this still holds in the limit of low particle numbers, i.e., when a full many-body description is required. Therefore, two different approaches are presented, where the previous results are applied to the many-body four-mode system in order to investigate if realizations of the two-mode model and $\mathcal{PT}$ symmetry are also feasible beyond the MF approximation.

A. Pure many-body states

First, we have to create the same initial condition for a many-body system; that is, we construct a pure many-body state from a MF state (9). To do so, an ansatz of identical single-particle wave functions is used, which can be written in terms of Fock states as

$$|\psi, N\rangle = \sum_{n_1,\ldots,n_M} u_{n_1,\ldots,n_M} |n_1, \ldots, n_M\rangle, \tag{25a}$$

with the sum running over all possible combinations with total particle number N. The coefficients are then given by

$$u_{n_1,\ldots,n_M} = \sqrt{N!} \prod_{m=1}^{M} \frac{\psi_m^{n_m}}{\sqrt{n_m!}}, \tag{25b}$$

where each component of the macroscopic wave function ψ_m is raised to the power of the corresponding population and normalized appropriately.

To obtain the representation of a pure many-body state also for the BBR approximation, we consider the action of the annihilation operator onto the state (25a),

$$\hat{a}_k |\psi, N\rangle = \sqrt{N}\psi_k |\psi, N-1\rangle, \tag{26}$$

which again yields a pure many-body state for $N-1$ particles. This leads to

$$\sigma_{ij}^{(1)} = N\psi_i^*\psi_j, \tag{27a}$$

$$\sigma_{ijkl}^{(2)} = N(N-1)\psi_i^*\psi_j\psi_k^*\psi_l + N\psi_i^*\delta_{jk}\psi_l. \tag{27b}$$

With Eqs. (25) and (27) we can now prepare the system in a pure state corresponding to MF states as in Eq. (9). In the following sections we will always assume that the four-mode system is prepared in an initial state corresponding to Eqs. (21). Such an initial state corresponds indeed to the ground state of the respective embedded two-mode system in the MF but is in general not the ground state of the many-body system itself.

B. Mean-field-like approach

The results of Sec. III are in agreement with Refs. [29,30] together with Eq. (11). We now want to go beyond the MF approximation by using the methods discussed in Sec. II for $M = 4$ in order to examine which many-body effects occur and whether $\mathcal{PT}$-symmetric stationary states can still be established. Since the BH model contains more degrees of freedom than the GPE, whereas there are at the same time no additional free control parameters, that problem is highly nontrivial.

There is another important difference between MF and many-body dynamics that we have to pay special attention to. Calculations for the two-mode model in the MF approximation are typically performed using $n_1 = n_2 = 1/2$. The reason is that the GPE only describes a single-particle dynamics and the total particle number $N_2 = n_1 + n_2$ is just a parameter, which can therefore be normalized to $N_2 = 1$. However, for the BH model and the BBR approximation, this is not the case anymore. To allow for a comparison with the open two-mode system (8), which is described in terms of the (normalized) macroscopic interaction strength g, the macroscopic interaction strength in the four-mode model g_4 has to be modified according to

$$g_4 = \frac{g}{N_2}. \tag{28}$$

The contact-interaction potential U for many-body calculations is then obtained from g_4 by using Eq. (10); that is, $U = g_4/(N-1)$.

Let us start in a pure many-body state (25) corresponding to Eqs. (21), i.e., in particular the relations (14) hold. We then introduce time-dependent parameters also in the BH model as in Sec. III. As a first attempt we try to impose the same conditions as in the MF. Thus, we can directly check the effects of many-particle corrections on the dynamics and whether $\mathcal{PT}$ symmetry can be implemented by using exactly the same conditions as in the MF.

First, we demand that the currents are given by the coupling strength γ which gives formally the same results for the tunneling rates as in Sec. III B, which implies that Eqs. (15) are also usable for the BH model with $\tilde{j}_{ij}^{(1)} = 2\,\mathrm{Im}\,\sigma_{ij}^{(1)}$.

Second, we evaluate $\dot{c}_{01}^{(1)} = \dot{c}_{23}^{(1)} = 0$ for the many-body dynamics where $c_{ij}^{(1)} = 2\,\mathrm{Re}\,\sigma_{ij}^{(1)}$. This yields

$$\mu_0(t) = \frac{\mathcal{Y}_{01}^{(1)}(t)}{\tilde{j}_{01}^{(1)}(t)} = -J_{12}\frac{\tilde{j}_{02}^{(1)}(t)}{\tilde{j}_{01}^{(1)}(t)} - U\frac{\tilde{j}_{0001}^{(2)}(t) - \tilde{j}_{0111}^{(2)}(t)}{\tilde{j}_{01}^{(1)}(t)}, \tag{29a}$$

$$\mu_3(t) = \frac{\mathcal{Y}_{23}^{(1)}(t)}{\tilde{j}_{23}^{(1)}(t)} = -J_{12}\frac{\tilde{j}_{13}^{(1)}(t)}{\tilde{j}_{23}^{(1)}(t)} + U\frac{\tilde{j}_{2223}^{(2)}(t) - \tilde{j}_{2333}^{(2)}(t)}{\tilde{j}_{23}^{(1)}(t)}, \tag{29b}$$

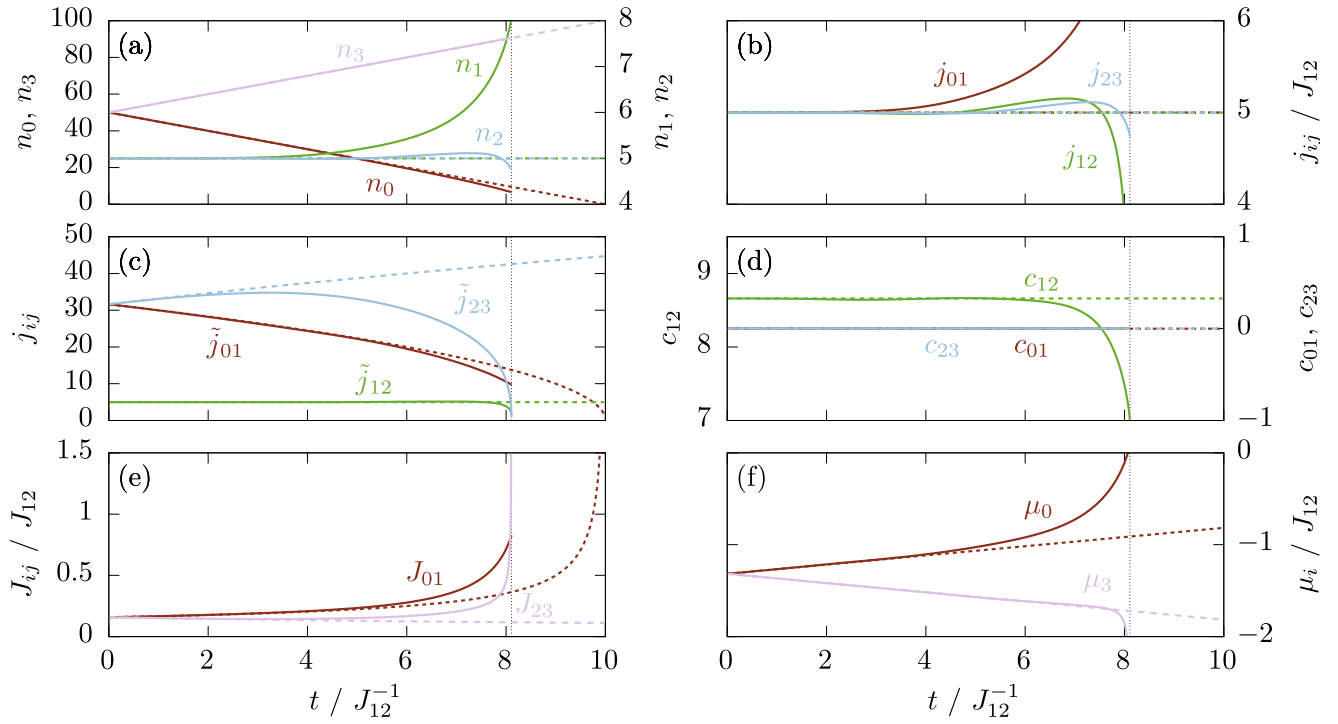

FIG. 2. Observables and parameters for a weakly interacting BEC with $g = 0.1$ described by the BH model. The coupling strength is fixed to $\gamma = 0.5$ and the occupation ratio between the embedded system and the reservoir is 10 for a total number of $N = 110$ particles. In comparison with the MF limit (dashed lines), the many-body system (solid lines) shows no quasistationary behavior, which is clearly visible by looking at (a) the occupation numbers n_1 and n_2, and the reduced current (b) $\tilde{j}_{12}$ and (d) c_{12}. The many-body calculations also show an earlier breakdown of the system (dotted vertical line) due to (c) $\tilde{j}_{23}$ dropping to zero, leading to (e) divergent tunneling rates and (f) on-site energies. Note that panels (a) and (d) have two separate vertical axes due to the different ranges of their observables.

where

$$\mathcal{Y}_{ij}^{(1)} = 2\,\mathrm{Im}\,\mathcal{Z}_{ij}^{(1)}. \tag{29c}$$

The first-order terms are now marked explicitly, since second-order terms corresponding to TPDMs are present; that is, $\tilde{j}_{ijkl}^{(2)} = 2\,\mathrm{Im}\,\sigma_{ijkl}^{(2)}$. In contrast to the MF parameters (19), the above equations contain corrections of second order due to a coupling of the equations of motion via interactions. At this point it should also be noted that the choice of parameters (29) can no longer fulfill the relations (14) except for perfectly pure states, that is only in the MF. Therefore, this approach should be viewed as an extension of the MF method in the vicinity of pure states.

In Fig. 2 the results of the many-body conditions (29) are shown in comparison with the MF limit discussed in Sec. III B for a weakly interacting BEC described by the BH model. The parameter $\gamma = 0.5$ is chosen in such a manner that the timescale (24) for the MF calculations reduces to the ratio of the initial occupations of the left reservoir and embedded system wells, $\tau = n_0/n_1$. In the MF (dashed lines) we clearly find stationary states in the embedded wells, which are in agreement with Refs. [29,30] and the analytical solutions from Eq. (20) [see especially Figs. 2(a)–2(b)]. The occupations in the reservoir wells change linearly in time as in Eqs. (22) and the parameters in Figs. 2(e) and 2(f) follow Eqs. (23). At $t = 10$ the calculation breaks down due to the left system well being empty and J_{01} thus diverges according to Eq. (15a).

In the MF, $\mathcal{PT}$ symmetry in the inner wells is realized by quasistationary states for the whole time interval $t \leqslant 10$; applying the same conditions to the many-body system yields a somewhat shorter timescale due to an earlier breakdown of the system at $t \sim 8$ without any well being completely empty. This breakdown is caused by the reduced current $\tilde{j}_{23}$ dropping to zero, which is a singularity in both J_{23} and μ_3 [see Eqs. (15b) and (29b)]. For $t \lesssim 2$, however, the many-body dynamics is in good agreement with the MF limit, showing approximately the same stationary behavior. This is reasonable, since we always start calculations with a pure state. However, eventually the dynamics of the many-body system evolves differently due to decoherence, thus not realizing quasistationary states anymore, as is clearly observable in Figs. 2(a)–2(d).

However, the differences between MF and many-body dynamics as well as the time of the breakdown strongly depend on the choice of parameters, in particular the total number of particles N and the contact-interaction strength g. If the ratio g/N becomes small, the influence of the many-particle contributions becomes insignificant and the MF description is good. The larger this ratio becomes, the earlier the many-particle dynamics will deviate from the stationary solutions and the system will break down.

It should be noted, that Eqs. (18) hold for all times [see Fig. 2(d)], since we demanded it reference to the conditions in the MF. Thus again, these conditions are only physically meaningful for balanced gain and loss in the vicinity of pure states and do not prevent the system from decoherence.

Instead, Eqs. (18) are maintained by a nonstationary many-body dynamics.

C. Realization of balanced gain and loss

To achieve true quasistationarity in the many-body system for $t \leqslant \tau$, which corresponds to exact $\mathcal{PT}$ symmetry in the related MF system, we have to demand that $\frac{\partial}{\partial t}\sigma_{12} = 0$, i.e.,

$$\mathrm{Re}\left(\frac{\partial}{\partial t}\sigma_{12}\right) = \frac{1}{2}\frac{\partial}{\partial t}c_{12}^{(1)} = 0, \tag{30a}$$

$$\mathrm{Im}\left(\frac{\partial}{\partial t}\sigma_{12}\right) = \frac{1}{2}\frac{\partial}{\partial t}\tilde{j}_{12}^{(1)} = 0. \tag{30b}$$

Since J_{12} is time independent, Eq. (30b) states that the current between the inner wells is constant, directly implicating stationary occupation numbers in said wells. In doing so one has to keep in mind that, in case of a many-body system, stationarity can only refer to the expectation values, since the variances only vanish completely in the MF limit. In fact, variances are closely connected to the higher-order terms in the BBGKY hierarchy,

$$\mathrm{var}\,(\hat{n}_i) = \Delta_{iiii}\,, \tag{31a}$$

$$\mathrm{var}(\hat{\tilde{j}}_{ij}) = \Delta_{ijji} + \Delta_{jiij} - \Delta_{ijij} - \Delta_{jiji}\,, \tag{31b}$$

$$\mathrm{var}(\hat{c}_{ij}) = \Delta_{ijji} + \Delta_{jiij} + \Delta_{ijij} + \Delta_{jiji}\,, \tag{31c}$$

where

$$\Delta_{ijkl} = \sigma_{ijkl}^{(2)} - \sigma_{ij}^{(1)}\sigma_{kl}^{(1)} \tag{31d}$$

are the covariances [27,28,32].

As one may easily confirm by using Eq. (8) that both Eqs. (30) are fulfilled in the MF limit at the same time by $n_1 = n_2$, i.e., they are dependent in the MF. In contrast, these equations are independent in the many-body case. This makes these conditions suitable to determine the on-site energies μ_0 and μ_3. Although this method should thus provide unique solutions for the parameters, the fact, however, that both conditions coincide for pure states renders any numerical calculation impossible. Equations (30) are linear equations in the parameter space (μ_0,μ_3) [cf. Eqs. (4)], therefore the unique solution is given by the intersection. In the vicinity of pure states, however, those lines are approximately parallel as outlined in Fig. 3. In this case the ability to accurately calculate the intersection point is lost due to numerical errors. Using these parameters in calculations will eventually destroy the dynamics after only a few iterations.

Obviously our approach does not allow for a realization of full quasistationarity in a many-body system with pure initial states, i.e., stationary expectation values in the embedded system, which again corresponds to $\mathcal{PT}$ symmetry in the MF limit; note, however, that this method should work for sufficiently impure states. Instead, we want to pursue the realization of BGL in the sense that there is a stationary, nonzero current expectation value between the inner wells [see Eq. (30b)]. This again leads to the conservation of the occupation expectation values in the embedded wells for a finite time, provided that the system is initially prepared in a state of the form Eq. (21). To achieve this, the on-site energies are modified according to Fig. 3, choosing a specific solution

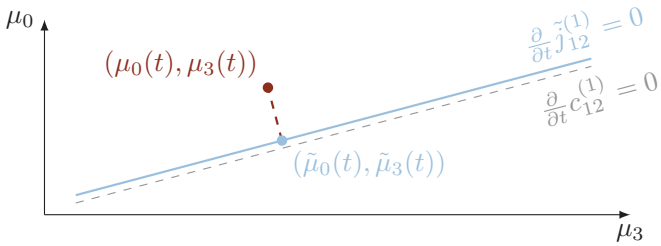

FIG. 3. Equations (30) in the vicinity of pure states. Since both lines are almost parallel, the unique solution cannot be calculated accurately. By projection of the parameters (29) onto the imaginary part yielding $(\tilde{\mu}_0,\tilde{\mu}_3)$, a constant particle flow between the inner wells is achieved. While in principle all points on the solid curve representing Eq. (30b) are valid, our approach stays as close as possible to the former approach adapted from the MF.

with stationary current which is closest to the parameters determined via Eqs. (29). The result is

$$\mu_0^{(1)} = \frac{\alpha\Omega + \beta^2\mu_0^{(0)} - \alpha\beta\mu_3^{(0)}}{\alpha^2+\beta^2}, \tag{32a}$$

$$\mu_3^{(1)} = \frac{\beta\Omega + \alpha^2\mu_3^{(0)} - \alpha\beta\mu_0^{(0)}}{\alpha^2+\beta^2}, \tag{32b}$$

where

$$\alpha = J_{01}\left(\tilde{j}_{02}^{(1)} + c_{02}^{(1)}\frac{c_{01}^{(1)}}{\tilde{j}_{01}^{(1)}}\right), \tag{32c}$$

$$\beta = J_{23}\left(\tilde{j}_{13}^{(1)} + c_{13}^{(1)}\frac{c_{23}^{(1)}}{\tilde{j}_{23}^{(1)}}\right), \tag{32d}$$

$$\begin{aligned}\Omega = {} & J_{01}c_{02}^{(1)}\frac{\mathcal{X}_{01}^{(1)}}{\tilde{j}_{01}^{(1)}} - J_{23}c_{13}^{(1)}\frac{\mathcal{X}_{23}^{(1)}}{\tilde{j}_{23}^{(1)}} \\ & + J_{01}\mathcal{Y}_{02}^{(1)} + J_{12}\left(\mathcal{Y}_{22}^{(1)} - \mathcal{Y}_{11}^{(1)}\right) - J_{23}\mathcal{Y}_{13}^{(1)} \\ & - U\left(\mathcal{Y}_{1112}^{(2)} - \mathcal{Y}_{1222}^{(2)}\right),\end{aligned} \tag{32e}$$

and

$$\mathcal{X}_{ij}^{(1)} = 2\,\mathrm{Re}\,\mathcal{Z}_{ij}^{(1)} \tag{32f}$$

is defined in analogy to Eq. (29c).

Since Eq. (30a) will not be fulfilled in general, i.e., $c_{12}^{(1)}$ is not stationary, this method does not reliably reproduce quasistationary states.

1. Low particle numbers

The dynamics obtained with these modifications for a relatively low total number of $N = 110$ particles is shown in Fig. 4 with the same initial conditions as in Fig. 2 and also in comparison with the MF dynamics. The many-body system again follows the MF dynamics on a small timescale $t \lesssim 2$ almost exactly and then deviates leading also in this case to an earlier breakdown than in the MF. However, for the whole timescale before the breakdown of the system both the occupation and current expectation values, i.e., n_1, n_2, and $\tilde{j}_{12}$, are preserved exactly, which can clearly be seen in Figs. 4(a)

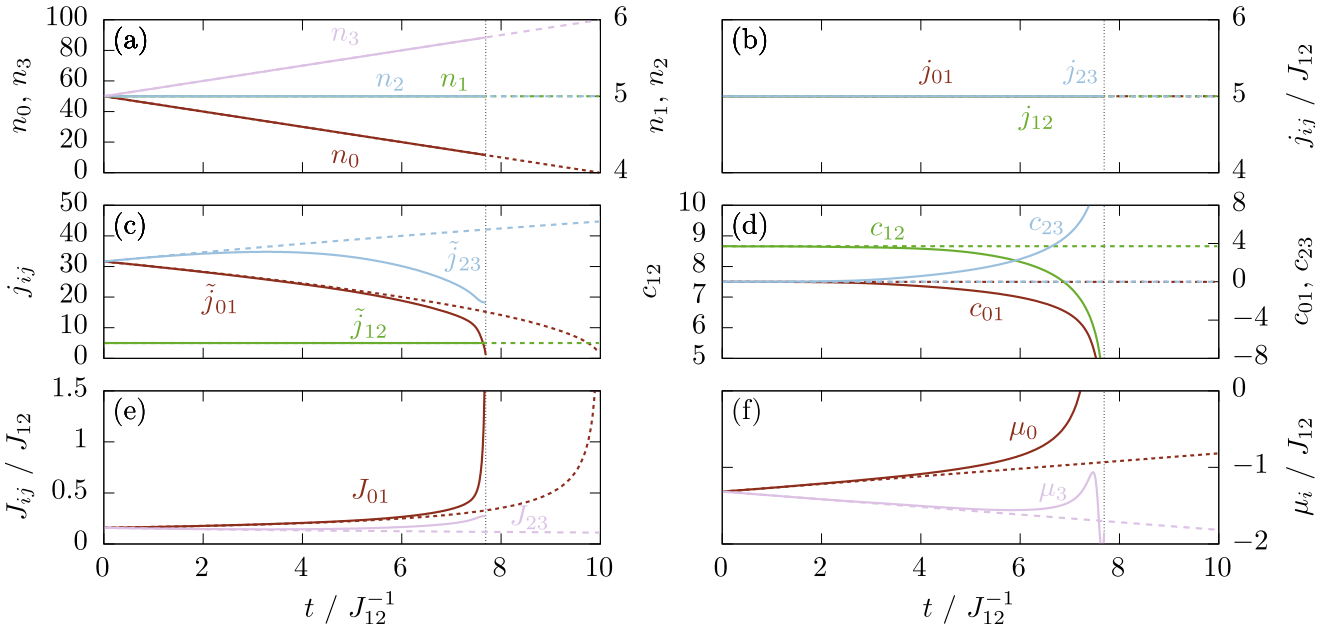

FIG. 4. Same as Fig. 2 but with modified on-site energies as shown in Fig. 3. The BH dynamics (solid lines) show (a) stationary occupation numbers in the embedded wells and (b) stationary currents between neighboring wells, which we call the BGL state. There is still an earlier breakdown in comparison with the MF dynamics (dashed lines), now caused by $\tilde{j}_{01}$ dropping to zero. (f) Due to the modifications (32), some parameters are no longer monotonic. Note that panels (a) and (d) have two separate vertical axes due to the different ranges of their observables.

and 4(b). It is remarkable that not only the quantities in the embedded system are in perfect agreement with the MF dynamics, but that the same also holds for all other occupation and current expectation values; this means that the occupation numbers in the reservoir change linearly in time and all current expectation values are equal and conserved; cf. Eqs. (20) and (22).

Apart from this, since $c_{12}(t)$ is explicitly time dependent and thus in general changes in time, the realized state is not truly quasistationary. That is, in a many-body system BGL, as we introduced it, will not induce quasistationarity by default anymore as it is the case in the MF. Nevertheless, these states will make a transition into true quasistationary states in the MF limit, i.e., $\mathcal{PT}$-symmetric states of the embedded system. It should be noted that, due to the modified on-site energies (32), the parameters may show more complex behavior, as can be seen for example in Fig. 4(f). Besides, the breakdown is, unlike before, now caused by the reduced current $\tilde{j}_{01}$ dropping to zero, as can be seen in Fig. 4(c), leading to singularities in J_{01} and μ_0 [see Eqs. (15a) and (29a)].

2. *Large particle numbers*

As discussed in Sec. II B, the computational effort for calculating exact BH dynamics increases rapidly with the total number of particles, restricting us to $N \lesssim 200$. To investigate systems with a total number of particles on the same order of magnitude as in typical experiments, i.e., $N \gtrsim 1000$, we use the BBR method introduced in Sec. II B. It should be noted at this point that the BBR approximation for $N \sim 200$ already shows excellent agreement with exact many-body calculations on the given timescale, therefore justifying its application for larger particle numbers.

Figure 5 shows a comparison between the two approaches from Figs. 2 and 4, but for $N = 1100$. For such large numbers of particles the relative deviations between the different many-body calculations become very small and the same holds for deviations from the MF dynamics. Nonetheless, the key differences are still observable, i.e., the system moves away from the BGL state after only few time steps without modification of the on-site energies. While these differences are quite prominent in the observables shown in Figs. 5(a)–5(d), i.e., the system evolves in a very distinctive manner in each case, it is rather surprising that there are only minor differences in the parameters shown in Fig. 5(e) for the most part of the time evolution. Only towards the breakdown of the system does the behavior change due to the divergent behavior; the modifications thus becoming more significant.

Using the reduced SPDM $\sigma_{\mathrm{red}}^{(1)}$ and the fact that it has only one macroscopic eigenvalue in case of a pure BEC, corresponding to a general criterion for Bose-Einstein condensation [50–53], we can define the purity [32] of an M-mode system by

$$P_M = \frac{M \operatorname{tr}\left(\sigma_{\mathrm{red}}^{(1)} \cdot \sigma_{\mathrm{red}}^{(1)}\right) - 1}{M - 1}. \tag{33}$$

This quantity is restricted to $[0,1]$, where $P_M = 1$ describes a perfectly pure BEC and $P_M = 0$ a maximally fractioned and thus impure BEC. Figure 5(f) shows the purities of the four-mode system P_4 and of the embedded two-mode system P_2 under the assumption that the embedded system effectively models an open quantum system. Also in this case the deviations between the original and the modified method remain small. Due to particle interactions, the coherence of the initial state is eventually destroyed [54], i.e., the purity of the system is reduced. On the one hand, it is remarkable that the purity of the embedded system drops only slightly at first despite the rather small number of $N_2 = 100$ particles, which is a consequence of the initial quasistationary state of

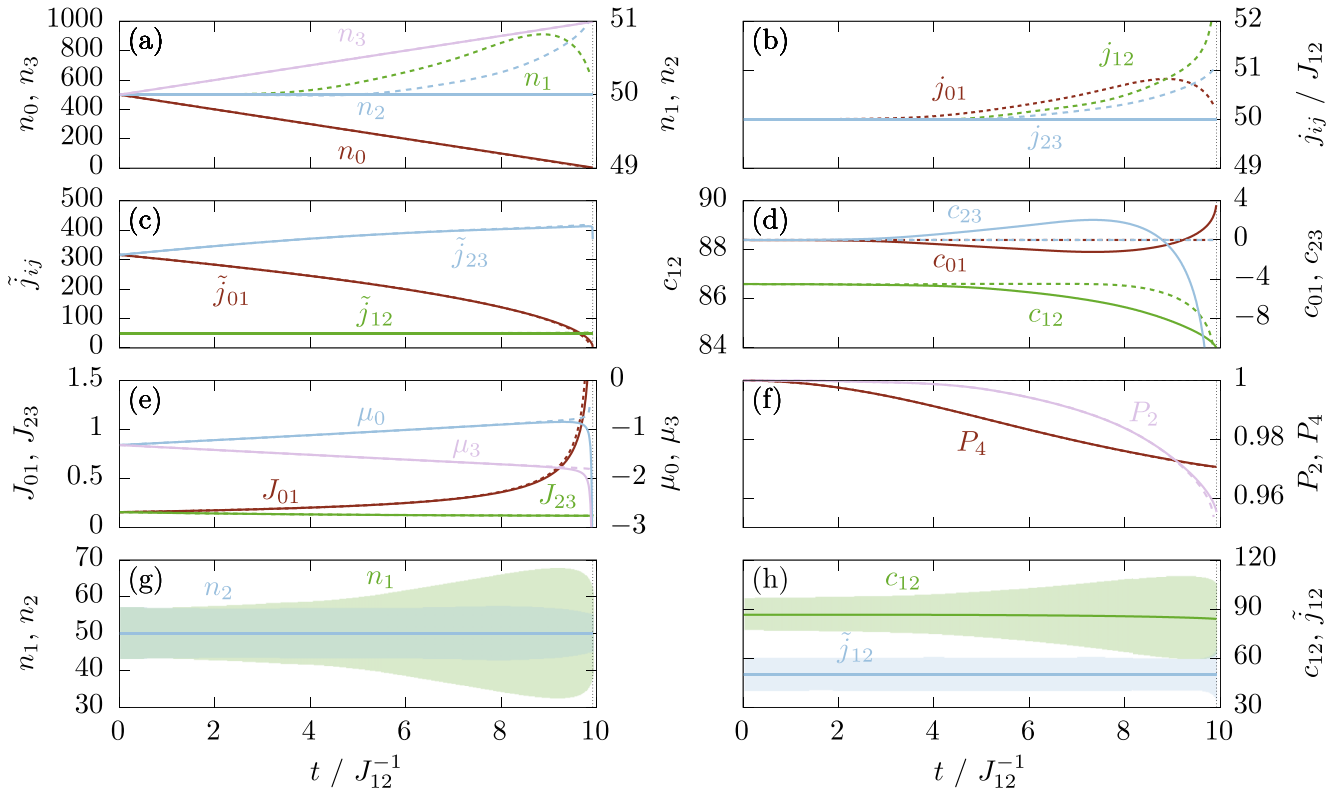

FIG. 5. Comparison of the first approach from Fig. 2 (dashed lines) with the second approach from Fig. 4 (solid lines) for a total number of 1100 particles with the same occupation ratio as before. Many-body calculations were performed within the BBR approximation. (a)–(d) Although the time of the breakdown (dotted vertical line) almost matches that of the MF limit in Figs. 2 and 4 (note that the calculation ends slightly before $t = 10$), there are still deviations from the MF dynamics; cf. Figs. 2 and 4. For both approaches the time-dependent parameters are in good agreement and only show different behavior close to the breakdown. (f) The same holds for the purities of the four-mode system P_4 and the embedded two-mode system P_2. (g), (h) The standard deviations for the embedded observables are shown for the BGL state. Note that panels (a), (d), and (e) have two separate vertical axes due to the different ranges of their observables.

the corresponding MF system [27,32]. On the other hand, this shows that BGL can be realized in the true many-body regime, in which most part of the simulation takes place.

Figures 5(g) and 5(h) show the observables of the embedded system for the modified on-site energies in the context of their respective variances (31). The variances are the same order of magnitude as the total particle number N, even though, for increasing N, the relative variances of the observables will shrink. More interesting, however, is the different behavior of the occupation number expectation values. The expectation values of n_1 and n_2 are conserved for the whole simulation time, and their variances are initially equal. Yet, we then find an overall growth of var (n_1) while var (n_2) remains approximately constant. Similar behavior is also visible for other one-particle expectation values such as the reduced currents between system and reservoir [55]. While such a growth of variances over time; that is, an increasing uncertainty, may be a consequence of the finite reservoir and the constraints due to the time-dependent parameters, it certainly is connected to the breakdown of the system caused by a singularity due to the vanishing of a reduced current expectation value.

However, even if time-dependent optical lattices are theoretically feasible and experimentally accessible for the control and realization of such systems, an experimental realization would be fundamentally different from the theoretical methods. In real experiments one would probably tune the parameters in a predefined way, such that the potential is only time dependent but not state dependent. That is, one has to determine the parameters by theory rather than by means of *in situ* measurements, which are collapsing the wave function and thus destroying the condensate immediately. In this way, the system will evolve unperturbed and can be measured at different times, so that comparing the observables to theoretical results in the limit of many realizations of the experiment is possible.

V. CONCLUSIONS

By means of time-dependent potentials in four-mode optical lattices, we investigated the possibilities of effectively describing pure two-mode BECs with gain and loss in the $\mathcal{PT}$-symmetric regime. Starting with the GPE for pure states in the MF limit we derived precise conditions leading to time-dependent parameters. To further investigate the few-body limit, we used exact time evolution to perform many-body calculations of our system. These simulations, however, show that the MF approach is not suitable in the many-body case and the system evolves into the $\mathcal{PT}$-broken regime albeit being in the $\mathcal{PT}$-symmetric regime at the beginning. As discussed in

Sec. IV C, we cannot achieve true quasistationarity by means of pure initial states.

Nevertheless, we realized what is probably the intuitive notion of BGL, i.e., a configuration where stationary populations and a constant particle flow are present for the whole simulation time. Yet, also in this case the system will break down at some point into a $\mathcal{PT}$-broken state. The creation of controlled gain and loss over such long timescales lays the foundation for experimental investigations of generic many-body quantum effects in BGL systems like the aforementioned purity oscillations [28,32,33].

We can further confirm with our system that exact nonoscillating $\mathcal{PT}$-symmetric pure states, which arise very naturally in the MF limit as the unique stationary solutions in an open quantum system, are an exclusive feature of the GPE, as previous many-body investigations of the two-mode model have already shown [27,33]. Although no true quasistationarity can be achieved for finite numbers of particles; that is, without the MF approximation, both approaches discussed in Sec. IV will make a transition into the $\mathcal{PT}$-symmetric four-mode model in the MF limit.

In the present work we used the minimum setup for the realization of reservoirs, i.e., only one reservoir well at each side, respectively. Although such a reservoir may behave approximately Markovian for a large number of particles, which can be investigated by using the BBR approximation, we still see prominent differences. Since every additional reservoir well is increasingly expensive in computational costs, a large number of reservoir wells cannot be treated without further approximation. In a future work these additional reservoir wells could be included into our many-body calculation by means of the MF limit. In this way, effects of the finite reservoir could be suppressed. Another improvement might be the inclusion of a real loss term as used in Refs. [23,26,49], rendering a reservoir at the out-coupling well unnecessary.

APPENDIX: LEXICOGRAPHIC HOPPING

To calculate BH dynamics, the Hamiltonian has to be applied directly by matrix multiplication, which means that the entries of the Hamiltonian matrix have to be calculated. While the potential part of the Hamiltonian (1) yields only diagonal elements, the kinetic terms are off-diagonal. Since the resulting matrix is extremely sparse, only the nonzero entries have to be calculated explicitly. This implies that one has to apply every creation-annihilation operator pair, i.e., the hopping terms, to each Fock state separately and find the index of the resulting state. Searching for specific Fock states in a large basis set is slowing down calculations considerably. We therefore present a method for efficiently calculating the state index in a lexicographically ordered Fock basis. Details about this method and its implementation can be found in Ref. [56].

The dimension of the entire Fock basis for N particles in M potential wells is given by

$$D(N,M) = \binom{N+M-1}{N}. \tag{A1}$$

All Fock states with $n_1 < N$ particles on the first site are part of a subspace with $\tilde{n} = N - n_1$ particles in $M-1$ sites. These $D(\tilde{n},M')$ states start at index

$$\nu(n_1) = \sum_{\tilde{n}=0}^{N-n_1-1} D(\tilde{n},M-1), \tag{A2}$$

such that the first Fock state with $n_1 = N$ occupies $\nu = 0$. For a Fock state $|n_1,\ldots,n_M\rangle$, we have to sum up over all sites, which eventually yields the global index

$$\nu(n_1,\ldots,n_M) = \sum_{m=1}^{M-1}\sum_{\tilde{n}=0}^{N_m-1} D(\tilde{n},M_m), \tag{A3}$$

where $N_m = N - \sum_{k=1}^{m} n_k$ and $M_m = M - m$. It should be noted that only the first $M-1$ occupation numbers are important, since the last one is included in the boundary condition $\sum_{m=1}^{M} n_m = N$.

The numerical effort can further be reduced when only the index shift between the Fock states before and after the application of a hopping term $\hat{a}_i^\dagger \hat{a}_j$ is calculated, which is given by

$$s_{ij} = \begin{cases} -\sum_{m=\tilde{m}}^{\tilde{M}-1} D(N_m-1,M_m), & n'_{\tilde{m}} > n_{\tilde{m}} \\ \sum_{m=\tilde{m}}^{\tilde{M}-1} D(N_m,M_m), & n'_{\tilde{m}} < n_{\tilde{m}}, \end{cases} \tag{A4}$$

with $\tilde{m} \equiv \min(i,j)$ and $\tilde{M} \equiv \max(i,j)$. Since the kinetic part of the BH model (1) only contains nearest-neighbor hops, Eq. (A4) reduces to the calculation of a single binomial coefficient. Non-nearest-neighbor hops on the other hand can be interpreted as a sequence of successive nearest-neighbor hops.

[1] N. Moiseyev, *Non-Hermitian Quantum Mechanics* (Cambridge University Press, Cambridge, UK, 2011).

[2] C. M. Bender and S. Boettcher, Phys. Rev. Lett. **80**, 5243 (1998).

[3] A. Guo, G. J. Salamo, D. Duchesne, R. Morandotti, M. Volatier-Ravat, V. Aimez, G. A. Siviloglou, and D. N. Christodoulides, Phys. Rev. Lett. **103**, 093902 (2009).

[4] C. E. Rüter, K. G. Makris, R. El-Ganainy, D. M. Christodoulides, M. Segev, and D. Kip, Nat. Phys. **6**, 192 (2010).

[5] B. Peng, S. K. Ozdemir, F. Lei, F. Monifi, M. Gianfreda, G. L. Long, S. Fan, F. Nori, C. M. Bender, and L. Yang, Nat. Phys. **10**, 394 (2014).

[6] S. Weimann, M. Kremer, Y. Plotnik, Y. Lumer, S. Nolte, K. G. Makris, M. Segev, M. C. Rechtsman, and A. Szameit, Nat. Mater. **16**, 433 (2016).

[7] S. Bittner, B. Dietz, U. Günther, H. L. Harney, M. Miski-Oglu, A. Richter, and F. Schäfer, Phys. Rev. Lett. **108**, 024101 (2012).

[8] J. Schindler, A. Li, M. C. Zheng, F. M. Ellis, and T. Kottos, Phys. Rev. A **84**, 040101 (2011).

[9] S. Klaiman, U. Günther, and N. Moiseyev, Phys. Rev. Lett. **101**, 080402 (2008).

[10] D. Dast, D. Haag, H. Cartarius, G. Wunner, R. Eichler, and J. Main, Fortschr. Phys. **61**, 124 (2013).

[11] D. Dast, D. Haag, H. Cartarius, J. Main, and G. Wunner, J. Phys. A: Math. Theor. **46**, 375301 (2013).

[12] D. Haag, D. Dast, A. Löhle, H. Cartarius, J. Main, and G. Wunner, Phys. Rev. A **89**, 023601 (2014).

[13] D. Dizdarevic, D. Dast, D. Haag, J. Main, H. Cartarius, and G. Wunner, Phys. Rev. A **91**, 033636 (2015).

[14] E.-M. Graefe, J. Phys. A: Math. Theor. **45**, 444015 (2012).

[15] Y. Shin, G.-B. Jo, M. Saba, T. A. Pasquini, W. Ketterle, and D. E. Pritchard, Phys. Rev. Lett. **95**, 170402 (2005).

[16] R. Gati, M. Albiez, J. Fölling, B. Hemmerling, and M. K. Oberthaler, Appl. Phys. B: Lasers Opt. **82**, 207 (2005).

[17] Y. Kagan, A. E. Muryshev, and G. V. Shlyapnikov, Phys. Rev. Lett. **81**, 933 (1998).

[18] G. Lindblad, Commun. Math. Phys. **48**, 119 (1976).

[19] N. P. Robins, C. Figl, M. Jeppesen, G. R. Dennis, and J. D. Close, Nat. Phys. **4**, 731 (2008).

[20] D. Döring, G. R. Dennis, N. P. Robins, M. Jeppesen, C. Figl, J. J. Hope, and J. D. Close, Phys. Rev. A **79**, 063630 (2009).

[21] T. Gericke, P. Wurtz, D. Reitz, T. Langen, and H. Ott, Nat. Phys. **4**, 949 (2008).

[22] P. Würtz, T. Langen, T. Gericke, A. Koglbauer, and H. Ott, Phys. Rev. Lett. **103**, 080404 (2009).

[23] G. Barontini, R. Labouvie, F. Stubenrauch, A. Vogler, V. Guarrera, and H. Ott, Phys. Rev. Lett. **110**, 035302 (2013).

[24] F. Single, H. Cartarius, G. Wunner, and J. Main, Phys. Rev. A **90**, 042123 (2014).

[25] R. Gutöhrlein, J. Schnabel, I. Iskandarov, H. Cartarius, J. Main, and G. Wunner, J. Phys. A: Math. Theor. **48**, 335302 (2015).

[26] R. Labouvie, B. Santra, S. Heun, and H. Ott, Phys. Rev. Lett. **116**, 235302 (2016).

[27] D. Dast, D. Haag, H. Cartarius, and G. Wunner, Phys. Rev. A **90**, 052120 (2014).

[28] D. Dast, D. Haag, H. Cartarius, J. Main, and G. Wunner, Phys. Rev. A **94**, 053601 (2016).

[29] M. Kreibich, J. Main, H. Cartarius, and G. Wunner, Phys. Rev. A **87**, 051601 (2013).

[30] M. Kreibich, J. Main, H. Cartarius, and G. Wunner, Phys. Rev. A **90**, 033630 (2014).

[31] M. Kreibich, J. Main, H. Cartarius, and G. Wunner, Phys. Rev. A **93**, 023624 (2016).

[32] D. Dast, D. Haag, H. Cartarius, and G. Wunner, Phys. Rev. A **93**, 033617 (2016).

[33] D. Dast, D. Haag, H. Cartarius, J. Main, and G. Wunner, Phys. Rev. A **96**, 023625 (2017).

[34] H. A. Gersch and G. C. Knollman, Phys. Rev. **129**, 959 (1963).

[35] D. Jaksch, C. Bruder, J. I. Cirac, C. W. Gardiner, and P. Zoller, Phys. Rev. Lett. **81**, 3108 (1998).

[36] H. Feshbach, Ann. Phys. (NY) **5**, 357 (1958).

[37] C. Chin, R. Grimm, P. Julienne, and E. Tiesinga, Rev. Mod. Phys. **82**, 1225 (2010).

[38] J. M. Zhang and R. X. Dong, Eur. J. Phys. **31**, 591 (2010).

[39] P. Pisarski, R. M. Jones, and R. J. Gooding, Phys. Rev. A **83**, 053608 (2011).

[40] E. P. Gross, Nuovo Cimento **20**, 454 (1961).

[41] L. P. Pitaevskii, Sov. Phys. JETP **13**, 451 (1961) [J. Exptl. Theoret. Phys. (U.S.S.R.) **40**, 646 (1961)].

[42] E. Heller, J. Chem. Phys. **75**, 2923 (1981).

[43] D. Huber and E. J. Heller, J. Chem. Phys. **87**, 5302 (1987).

[44] E. M. Graefe, H. J. Korsch, and A. E. Niederle, Phys. Rev. Lett. **101**, 150408 (2008).

[45] A. Vardi and J. R. Anglin, Phys. Rev. Lett. **86**, 568 (2001).

[46] J. R. Anglin and A. Vardi, Phys. Rev. A **64**, 013605 (2001).

[47] I. Tikhonenkov, J. R. Anglin, and A. Vardi, Phys. Rev. A **75**, 013613 (2007).

[48] K. Henderson, C. Ryu, C. MacCormick, and M. G. Boshier, New J. Phys. **11**, 043030 (2009).

[49] B. Santra and H. Ott, J. Phys. B: At., Mol. Opt. Phys. **48**, 122001 (2015).

[50] O. Penrose, Philos. Mag. **42**, 1373 (2009).

[51] L. D. Landau and E. M. Lifshitz, *Statistical Physics* (Pergamon, Oxford, 1958).

[52] O. Penrose and L. Onsager, Phys. Rev. **104**, 576 (1956).

[53] C. N. Yang, Rev. Mod. Phys. **34**, 694 (1962).

[54] J. Ruostekoski and D. F. Walls, Phys. Rev. A **58**, R50 (1998).

[55] D. Dizdarevic, Master's thesis, Universität Stuttgart, 2016, doi:10.18419/opus-9175.

[56] K. Alpin, Bachelor's thesis, Universität Stuttgart, 2016, doi:10.18419/opus-8889.